

# Hard Pomeron Enhanced Cascade Production and Flux Shadowing in High-Energy Neutrino Astrophysics

A. Z. Gazizov\* and S. I. Yanush†

B. I. Stepanov Institute of Physics  
of the National Academy of Sciences of Belarus,  
F. Skariny Ave. 68, 220072 Minsk, Belarus

## Abstract

Various implications of new, non-perturbative pomeron inspired enhancement of small- $x$  neutrino-nucleon structure functions for high-energy neutrino astrophysics are discussed. At  $x \gtrsim 10^{-5}$  these functions are given by perturbative  $QCD$ , while at lower  $x$  they are determined by a specific generalization of  $F_2^{ep}(x, Q^2)$  description, proposed by A. Donnachie and P. V. Landshoff (their two-component model comprises *hard* and *soft* pomerons), to  $\nu N$ -scattering case.

We found that i) such enhancement causes the most rapid growth of  $\nu N$ -cross-sections at high energies, ii) that pomeron effects may be perceptible in the rates of neutrino induced events in future giant detectors and iii) that the rate of high-energy neutrino flux evolution (due to absorption ( $CC + NC$ ) and regeneration ( $NC$ )) on its pass through a large column depth of matter may be subjected to additional influence of hard pomeron. Solving transport equations for the initially power-law decreasing  $\nu$ -spectra, we have evaluated shadow factors for several column depths and spectrum

---

\*gazizov@dragon.bas-net.by

†yanush@dragon.bas-net.by

indices. The results are compared with analogous calculations, performed within a trivial small- $x$  extrapolation of structure functions. Hard pomeron enhanced high-energy shadow factors are found to be many orders of magnitude lower than those obtained within ordinary perturbative  $QCD$ .

## 1 Introduction

As a rule, accelerator experiments provide data of very high quality. But such measurements seem to be hardly possible at energies,  $E \gtrsim 1 \times 10^{19}$  eV, even in the very distant future.

On the other hand, *non-accelerator*, observational physics gives a good chance to get data at ultrahigh energies [1]. But the accuracy of data in this case is worse due to scarcer statistics and lower resolution of detectors. It is remarkable, that non-accelerator *High-Energy (HE)* physics combines into one the 'telescope' and 'microscope' physics. Really, the detected *UltraHigh-Energy (UHE)* particles are produced in perhaps most distant, extragalactic cosmic sources. Hence, it deals with extremely large, cosmological, distances. On the other hand, interactions of such particles with matter occur at least distances.

Realization of *UHE* astrophysics is a complex problem. It poses many hard questions, such as:

1. what types of ultrahigh-energy particles may be observed?
2. where and how ultrahigh-energy particles are produced?
3. what detectors are to be used?
4. what is the expected rate of events in a detector?
5. does this rate exceed the background?

Let us try to answer these questions in brief.

### 1.1 Particles

Through the centuries people used only star light, viz. optic photons, for the sky observation. Today actually the whole range of e.m. radiation, up to TeV photons [2], is involved in measurements.

Another well-known example of high-energy cosmic radiation is provided by Cosmic Rays (*CRs*). These are mostly protons ( $H$ ),  $He$ ,  $C$ ,  $N$  and up to  $Fe$  ions, which continuously bombard the atmosphere. Energy

spectrum of *CRs* extends from 1 GeV up to perhaps  $1 \times 10^{21}$  eV; the highest energy event with  $E \simeq 3 \times 10^{20}$  eV has been detected by the *AGASA* array [3]. The nature of incident particles in such events as well as where and how they are produced is unknown. Moreover, the average path length of  $E \gtrsim 6 \times 10^{19}$  eV protons in the cosmic microwave background radiation (with temperature  $T = 2.73K$ ) is essentially limited by  $p + \gamma \rightarrow \pi^+ + n$  interactions [4] (*GZK* cut-off), so that their presence in *CRs* is a problem.

Besides traditional photons and *CRs*, gravitation waves and neutrinos are also regarded as possible instruments for *HE* astrophysics. In this paper we concentrate on neutrinos, in particular, on *UHE* neutrinos with  $E_\nu \gtrsim 1 \times 10^{-15}$  eV. Being neutral, they do not deflect in magnetic fields, hence their arrival directions shoot back to the production site. Small cross-sections allow these neutrinos to travel extremely large distances without absorption. But their production in cosmic sources is difficult (i.e. sources are rare) and these sources are distant. It makes the expected flux to be small. Moreover, detection of such neutrinos is complicated by the same small cross-sections. To compensate for these negative factors, one should construct gigantic detectors.

## 1.2 Production

There are many theoretical models predicting large luminosity of cosmic sources in high-energy particles, including neutrinos (see e.g. [1]). For example, such fluxes may be produced in supernova explosions, in active galactic nuclei, during gamma-ray bursts etc. Energy outburst in these sources, including in the form of *HE* particles, may be really high, but the expected flux at the Earth remains low due to large distance.

Basically, there are two models of *HE* particle production. First assumes proton acceleration up to very high energies on cosmic source shocks (usually gas accretion onto a massive black hole, presumably residing in center of an active galaxy, is suggested), sometimes in relativistic jets pointing to the Earth. Then pions and kaons appear as a result of *pp*- and/or *p $\gamma$* -collisions in a source. These mesons decay, giving birth to *HE* neutrinos. The described scenario is called *down-top* mechanism. Unfortunately, it is difficult to obtain proton energies higher than  $E \sim 10^{17}$  eV in this mechanism; one needs both large shock radius and high magnetic field.

Another possibility is proposed by the *top-down* mechanism (for review and discussion of upper limits to the expected  $\nu$ -fluxes see e.g. Ref. [5] and

references therein). It is based on suggestion that some yet unknown, extremely massive (with  $m_X \sim 10^{14} \div 10^{16}$  GeV) long-living gauge  $X$ -bosons decay to the ordinary particles. These bosons allegedly originate from topological defects, which in their turn have been produced during a hypothetical phase transition in the early Universe. A big fraction of  $X$ -boson's energy goes to  $HE$  particles (neutrinos). These attractive models involve new physics beyond Standard Model and seem a bit speculative. An experimental verification is needed.

### 1.3 Detectors

$HE$  neutrino detectors should be very large and well shielded from background radiations. They are to have either  $S \gtrsim 1$  km<sup>2</sup>, especially if secondary muons (say from  $\nu_\mu + N \rightarrow \mu^- + X$ ) are detected, and/or gigantic mass,  $M \gtrsim 1 \times 10^9$  ton, in the case of registration using nuclear-electromagnetic cascades (from hadron state  $X$  in the  $\nu_\mu$  case or from  $\nu_e + N \rightarrow X$ ). These requirements may be met:

- by search for Cerenkov radiation in deep underwater detectors with desirable volume under control  $V \sim 1$  km<sup>3</sup> (mass  $M \sim 10^9$  ton);
- by registration of air nitrogen fluorescence, induced by Extended Air Showers; an effective control over  $M \sim 10^{11}$  ton of atmosphere may be achieved either from the earth (see Fly's Eye [6] and HiRes [7]) or from satellites (Airwatch [8] etc);
- using such a 'neutrino' detector, as *Pierre Auger* installation<sup>1</sup> [9]. Note, that *Pierre Auger* telescope is designed for the study of  $CRs$  at  $E > 1 \times 10^{20}$  eV, high-energy neutrino physics being just a byproduct.

### 1.4 Rate of events

The rate of nucleon-electromagnetic cascades in a neutrino detector is proportional to convolution product of  $\nu N$ -cross-sections and  $\nu$ -fluxes, and also to the number of scattering centers, i.e. mass of detector. A standard requirement is to have at least 10 events per year, but the only way to

---

<sup>1</sup>A hybrid detector in Argentina will consist of 1600 tanks, each filled with 12 m<sup>3</sup> of water. Stations will be distributed in a grid with 1.5 km spacing. b) Four *Fly's Eye* type fluorescence detectors, controlling  $\sim 3000$  km<sup>2</sup> of the site.

gain higher statistics is to increase the installation mass. But huge arrays are very expensive. However, the higher are  $\nu N$ -cross-section, the higher is the expected rate of events, the better results may be obtained.

## 1.5 Background

A severe problem for *HENA* is high *CR* background. One is to shield a detector either burying it deep underground (underwater, underice) or selecting just down-up going events, using the Earth as a shield. In any case, the atmospheric neutrino background (mostly from prompt  $\nu$ 's) is inevitable. Nevertheless, many  $\nu$ -source models suggest that extragalactic diffuse  $\nu$ -flux dominates at  $E \gtrsim 10^{15} \div 10^{17}$  eV.

## 1.6 The aims of the paper

We shall discuss several consequences for *HENA* of accelerated growth of neutrino-nucleon cross-sections at extremely high energies. We argue that such acceleration may be induced by non-perturbative hard pomeron with intercept  $\sim 1.4$ , which was proposed and successfully exploited in series of recent papers by A. Donnachie and P. V. Landshoff [17]. We study its influence on the rate of cascades in a  $\nu$ -detector and on evolution of neutrino spectra during their pass through large column depths of matter.

## 2 Cross-sections

Neutrino-nucleon scatterings proceed via *CC* and *NC* interactions:

$$\nu_l(\bar{\nu}_l) + N \rightarrow l^\mp + X, \quad (CC) \quad (1)$$

$$\nu_l(\bar{\nu}_l) + N \rightarrow \nu_l(\bar{\nu}_l) + X, \quad (NC) \quad (2)$$

where  $l = e, \mu, \tau$ . High energy behavior of  $\nu N$ -cross-sections is yet unknown. All attempts to estimate them at  $E \gtrsim 1$  TeV are mostly based on different extrapolations of nucleon *Structure Functions (SFs)*  $F_2^{\nu N}(x, Q^2)$ ,  $F_3^{\nu N}(x, Q^2)$  to  $x \lesssim 1 \times 10^{-5}$  (see e.g. Ref.s [10, 11, 12, 13]). In papers [14, 15] a new parameterization of these *SFs* has been derived. It was grounded on a successful description of  $F_2^{ep}(x, Q^2)$  by A. Donnachie and P. V. Landshoff [17], which claimed that small- $x$  *ep*-scattering data of *HERA* [16] may be successfully explained with the help of a simple combination

of several Regge theory inspired leading pole terms. The most important were so-called 'soft' (with intercept  $\sim 1.08$ ) and 'hard' (with intercept  $\sim 1.4$ , hence very similar to the perturbative *BFKL* one [18]) pomerons; first prevails at small  $Q^2$ , while the latter dominates at large  $Q^2$ . Moreover, *DL* argued that perturbative *QCD* (*pQCD*) fails at small  $x < 10^{-5}$  and even that its validity at  $x \sim 10^{-4} \div 10^{-5}$  is a pure fluke. However, the *DL* approach is also just a model, neglecting, in particular, all non-leading poles and cuts in the complex angular momentum  $l$ -plane. This results in violation of unitarity and unlimited growth of cross-sections at  $E_\nu \rightarrow \infty$ .

Using generalization of *DL*  $F_2^{ep}(x, Q^2)$  description to  $\nu N$ -scattering case, *SFs*  $F_2^{\nu N}(x, Q^2)$  and  $F_3^{\nu N}(x, Q^2)$ , presumably valid in the whole range of kinematic variables  $0 \leq x \leq 1$  and  $0 \leq Q^2 \leq \infty$ , have been derived in Ref. [15]. At  $x \gtrsim 10^{-5}$  they were determined by *pQCD* parameterization *CTEQ5* [19], while in the small- $x$  region they were driven by the analogous Regge theory inspired description. A special interpolation procedure have allowed to meet smoothly these different, both over  $x$  and  $Q^2$ , descriptions of *SFs* at low and high  $x$ . In Ref. [14] these new *SFs* were denoted by *DL+CTEQ5* indicating that they had their origin in the interpolation between *DL* and *pQCD* descriptions.

In parallel there were considered in Ref. [15]  $\nu N$  *SFs*, which had been derived by a simple extrapolation of *pQCD* *SFs* from  $x \geq 1 \times 10^{-5}$  to the small- $x$  region. These were given by formula:

$$F_i^{\nu N, \text{Log+CTEQ5}}(x < x_{min}, Q^2) = F_i^{\nu N, \text{CTEQ5}}(x_{min}, Q^2) \left( \frac{x}{x_{min}} \right)^{\beta_i(Q^2)}, \quad (3)$$

$$\beta_i(Q^2) = \left. \frac{\partial \ln F_i^{\nu N, \text{CTEQ5}}(x, Q^2)}{\partial \ln x} \right|_{x=x_{min}}; \quad x_{min} = 1 \times 10^{-5}, \quad (4)$$

$i = 2, 3$ . These *SFs* smoothly shot to the low- $x$  region from the *CTEQ5* defined high- $x$  one [10, 14, 15]. Starting values of functions and of their logarithmic derivatives over  $\ln x$  had been taken at the  $x = x_{min}$  boundary of *CTEQ5*. This parameterization was designated by *Log+CTEQ5*. Actually, these *SFs* are very close to analogous of Ref. [11].

Denoted as *DL+CTEQ5*, total *CC* + *NC*  $\nu N$ -cross-sections are shown in Fig. 1. For comparison there are also plotted the corresponding cross-sections, which were obtained

**a)** in the framework of simple *Log + CTEQ5* extrapolation (3);

- b) with the help of *CTEQ4* parameterization by *Gandhi et al.* Ref. [11], denoted as *GQRS-98 (CTEQ4)*;
- c) within a united *BFKL/DGLAP* approach by *Kwiecinski, Martin and Stasto* [13], labelled as *KMS*.

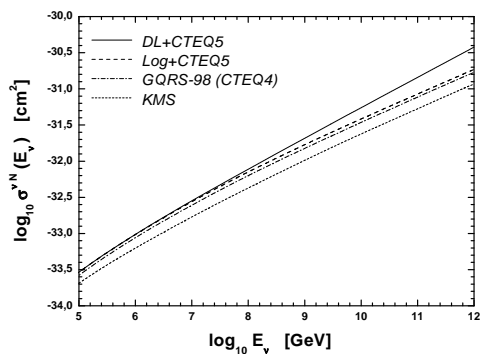


Figure 1: Total (*CC+NC*)  $\nu N$ -cross-sections. Labelling of the curves is described in the text.

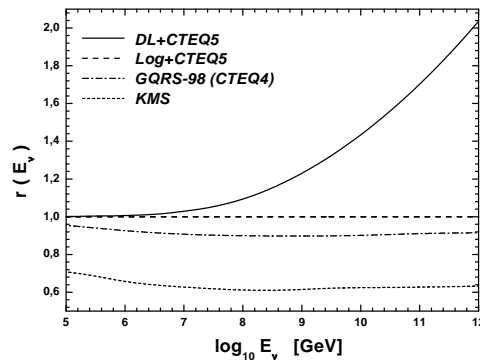


Figure 2:  $r(E_\nu)$  are ratios between cross-sections shown in Fig. 1 and the *Log+CTEQ5* cross-section.

Due to hard pomeron, our model predicts the most rapid growth of cross-sections at high energies. The differences between cited calculations become especially clear in Fig. 2, where each cross-section is divided by the cross-section of *Log+CTEQ5*.

### 3 Rates of cascades in $\nu$ -detectors

In this section we shall check the manifestations of pomerons in the rates of nuclear-electromagnetic cascades in deep underwater/underice detectors. To simplify the problem, we shall deal with an incident  $\nu$ -flux energy spectrum, approximated by a simple power-law decreasing function,

$$F_\nu(E_\nu, \gamma) = A \times E_\nu^{-(\gamma+1)}, \quad (5)$$

where  $\gamma$  is the index of an integral neutrino spectrum,  $F_\nu(> E, \gamma)^2$ , and  $A$  is the normalization coefficient. Most source models commonly assume  $1.1 \leq \gamma \leq 2.1$ . The real generation  $\nu$ -spectrum should be cut-off at high

<sup>2</sup> Note that for power-law spectra  $\gamma \times F_\nu(> E, \gamma) = E \times F_\nu(E, \gamma)$ .

energies of course, though in top-down models this may occur only at very large energy. Moreover, as it will be shown later, the high-energy part of neutrino spectrum suffers from attenuation on passage through large column depths of matter. Nevertheless, for the purposes of present consideration all these details may be temporarily neglected.

So, in the case of power-law decreasing spectra (5), differential and integral rates of cascade production in a detector may be calculated with the help of so-called demensionless differential,

$$Z_h(E_h, \gamma) = \int_0^1 dy y^\gamma \frac{d\sigma_{\nu N}(E_h/y, y)}{\sigma_0 dy}, \quad (6)$$

and integral,

$$Y_h(E_h, \gamma) = \gamma \int_0^1 du u^{\gamma-1} Z_h\left(\frac{E_h}{u}, \gamma\right), \quad (7)$$

hadron moments [20, 21]. Here  $E_h$  is the energy of a hadron-electromagnetic cascade,  $y = E_h/E_\nu$ , and  $\sigma_0 = G_F^2 m_W^2/\pi$  is the normalization cross-section (for  $m_W = 81$  GeV  $\sigma_0 = 1.09 \times 10^{-34}$  cm<sup>2</sup>). These rates in the case of  $CC$ -scattering (1) are

$$dN_h(E_h)/dt = Z_h^{CC}(E_h, \gamma) N_N \sigma_0 \Omega F_\nu(E_h), \quad (8)$$

$$dN_h(> E_h)/dt = Y_h^{CC}(E_h, \gamma) N_N \sigma_0 \Omega F_\nu(> E_h), \quad (9)$$

where  $N_N$  is the number of nucleons in a detector,  $\Omega$  is the effective solid angle, opened for the neutrino flux. To take into account the  $\bar{\nu}N$ - and  $NC$ -interaction cases, one should just substitute the appropriate differential cross-sections in the Eq. (6) for the  $CC$  cross-section.

In the case of electron (anti)neutrino  $CC$ -scattering (1) the role of differential hadron moment belongs to the corresponding normalized  $CC$ -cross-section,  $\sigma_{\nu_e N}^{CC}(E_\nu)/\sigma_0$ ; since here  $E_h = E_\nu$ , the  $\nu_e$ -flux in (8,9) is to be taken at the energy of incident neutrino.

According to Eq.s (6,7), hadron moments are sensitive to the high-energy parts of  $\nu$ -spectra. As a consequence, hard pomeron effects look even more pronounced in these observables. To illustrate a common trend of hadron moments, the differential and integral  $\nu N$  and  $\bar{\nu}N$  hadron moments are plotted in Fig. 3 and Fig. 4, respectively, for  $DL+CTEQ5$  parameterization and  $\gamma = 1.1$ , both for  $CC$  and  $NC$ .



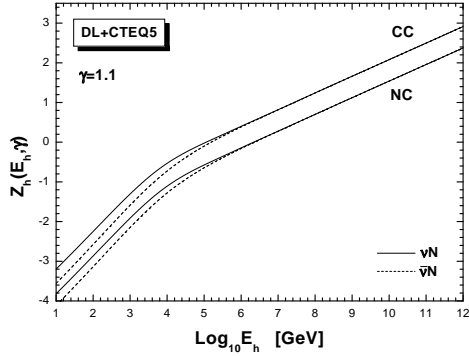


Figure 3: Differential  $CC$  and  $NC$  hadron moments for  $\gamma = 1.1$ .

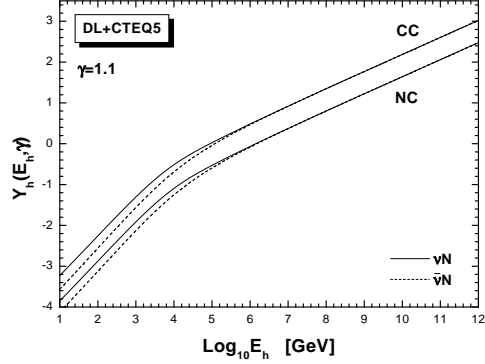


Figure 4: Integral  $CC$  and  $NC$  hadron moments for  $\gamma = 1.1$ .

A detailed discussion of dependencies of hadron moments on  $\gamma$  can be found in Ref. [22].

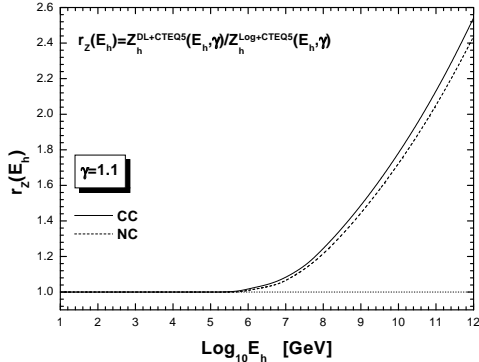


Figure 5: Ratios between  $CC$  differential hadron moments of  $DL+CTEQ5$  and  $Log+CTEQ5$  parameterizations for  $\gamma = 1.1$ .

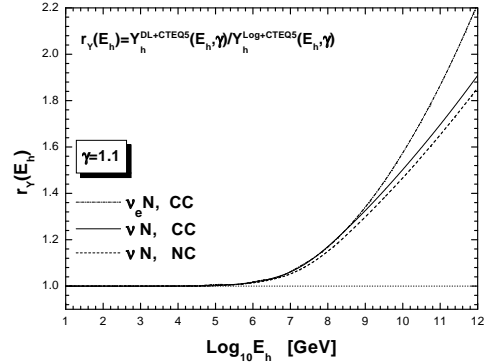


Figure 6: Analogous to Fig. 5 ratios of integral moments. The curve denoted  $\nu_e N$  describes the case of  $E_h = E_\nu$ .

It is informative to plot ratios between corresponding  $CC$  hadron moments, evaluated within  $DL+CTEQ5$  and  $Log+CTEQ5$  parameterizations, respectively. They are shown in Figs 5,6 for  $\gamma = 1.1$ . These figures corroborate our suggestion, that hadron moments are more sensitive to the non-perturbative pomeron effects. The strongest effect in integral moments takes place for  $\nu_e(\bar{\nu}_e)N$   $CC$ -scattering, when the whole energy of

the incident neutrino is transferred into cascade.

## 4 Absorption and regeneration of neutrino fluxes in matter

Neutrinos are known to be weak interacting particles. However,  $HE$  neutrinos should be absorbed in large dense samples of matter, when  $\sigma_{\nu N}(E) \times n \times l/m_N \gtrsim 1$ ; here  $n$  (in  $g/cm^3$ ) is the matter density and  $l$  (in  $cm$ ) is the range of neutrino pass. An appropriate variable for such consideration is column depth,  $\tau = n \times l$  (measured in  $g/cm^2$ ).

Attenuation effects may be described by a shadow factor, which is a ratio of neutrino flux at column depth  $\tau$  and the primary flux (i.e. at  $\tau = 0$ ):

$$S(E, \tau) = \frac{F_\nu(E, \tau)}{F_\nu(E, 0)}. \quad (10)$$

To a first approximation, shadow factor  $S(E, \tau) \approx \exp(-\sigma^{CC+NC}(E)\tau/m_N)$ . It provides an estimate that neutrinos with  $E > 10$  TeV (see Fig. 1), passing through the center of the Earth (column depth of matter in this case is  $\tau \simeq 1.1 \times 10^{10} g/cm^2$ ), are partially absorbed.

⊕ On the one hand, the higher is the energy, the stronger is attenuation. On the other hand, Earth is the natural, but not the unique example of a large column depth of matter in the Universe. One can easily imagine different environments with much higher column depths, where neutrino flux attenuations would be stronger as well. Hence, attenuation effects should be taken into account in *HENA*.

In this section we emphasize that hard pomeron enhanced  $\nu N$ -cross-sections bring to much higher attenuations of neutrino fluxes, than it was previously expected.

The absorption of neutrinos in the Earth have been earlier discussed by many authors. However, only in paper [10] the regeneration of neutrino fluxes due to  $NC$ -scattering (2) has been taken into account for the first time. To evaluate the effect, a 'thin target' model have been used in that paper. That model assumed that average attenuation length in the Earth is comparable with its diameter. And that was the case for the Earth as a target and the energy range considered in Ref. [10].

Nevertheless, in order to treat correctly the higher energies and larger column depths, a more sophisticated consideration is necessary. Ten years

later it was proposed by A. Nicolaidis and A. Taramopoulos in Ref. [23]. They have derived a trivial transport equation

$$\frac{d}{d\tau}F_\nu(E_\nu, \tau) = -\sigma^{CC+NC}(E_\nu) \times F_\nu(E_\nu, \tau) + \int_0^1 \frac{dy}{1-y} \times \frac{d\sigma^{NC}(E_\nu/(1-y), y)}{dy} \times F_\nu(E_\nu/(1-y), \tau) \quad (11)$$

and solved it (unfortunately, under some wrong assumptions about differential cross-sections). First term in the r.h.s. of the Eq. (11) accounts for the absorption, while the second one describes regeneration via  $NC$ .

Later these equations have been solved correctly by many authors with various parameterizations of high-energy  $\nu N$ -cross-sections (see e.g. Ref.s [11, 13]).

An elegant method for solution of the transport equation (11), along with a detailed discussion of different neutrino spectra evolution, has been given by V. A. Naumov and L. Perrone in paper [24]. In this paper we exploited their method, applying it to the infinite incident power-law decreasing neutrino spectra (5). Calculations were performed for the two parameterizations of differential cross-sections, viz. for  $DL + CTEQ5$  and  $Log + CTEQ5$ .

Our results are demonstrated in Figs 7-10.

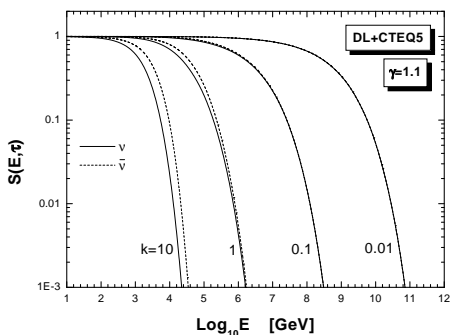


Figure 7: Shadow factors for  $\nu N$ - and  $\bar{\nu}N$ -scattering for several values of column depth, parameterized by the factor  $k = \tau/\tau_{\oplus}$ ;  $\tau_{\oplus} = 1.1 \times 10^{10} \text{g/cm}^2$  corresponds to the passage through the center of the Earth.

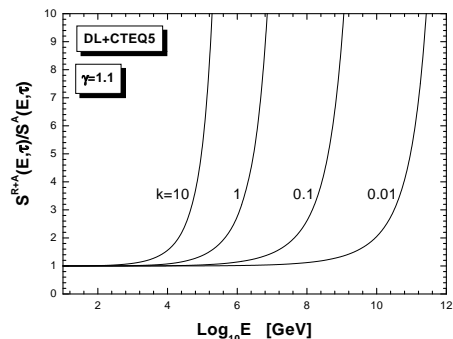


Figure 8: Ratios of  $\nu N$ -scattering shadow factors calculated with and without regard for regeneration of  $\nu$ -fluxes by neutral currents. Factors  $k$  are the same as in Fig. 7.

In Fig. 7 shadow factors  $S(E, \tau)$  (10), evaluated with the help of hard pomeron enhanced parameterization  $DL + CTEQ5$ , are plotted for neutrinos and antineutrinos. All curves relate to only one value of initial neutrino spectrum index,  $\gamma = 1.1$ . Evolution is illustrated by successively increasing values of column depth  $\tau$ , which are expressed in terms of the 'standard' column depth  $\tau_{\oplus} = 1.1 \times 10^{10} \text{g/cm}^2$ .

In Fig. 8 the importance of the regeneration term is emphasized. The ratios of shadow factors with regeneration and those accounting only for absorption are shown here for the same successively increasing column depths  $\tau$  as in Fig. 7.

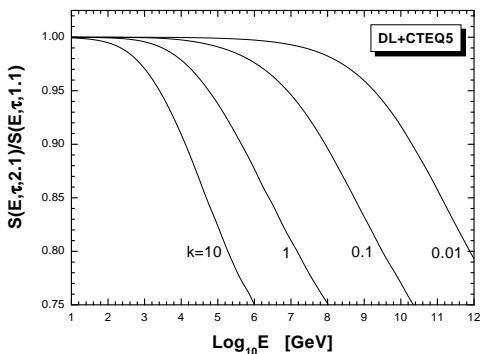


Figure 9: Ratios of  $\nu N$  shadow factors for incident  $\nu$ -spectra with indices  $\gamma = 2.1$  and  $\gamma = 1.1$ , respectively. Factors  $k$  are the same as in Fig. 7.

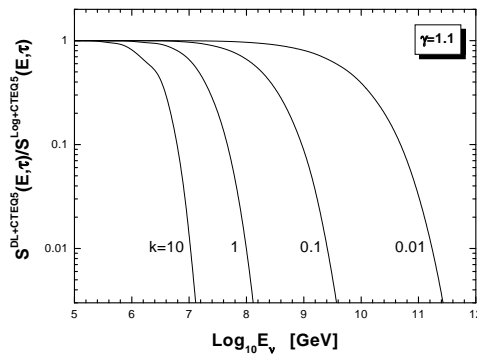


Figure 10: Ratios of  $\nu N$  shadow factors, calculated within  $DL + CTEQ5$  and  $Log + CTEQ5$  parameterizations, respectively. Factors  $k$  are the same as in Fig. 7.

The dependencies of shadow factors on  $\gamma$  may be understood from Fig. 9. The ratios of these factors are plotted here for two indices of initial spectra, viz.  $\gamma = 2.1$  and  $\gamma = 1.1$ . Evolution is shown in the same way as it was done in the previous figures.

And, finally, the ratios of shadow factors calculated within  $DL + CTEQ5$  and  $Log + CTEQ5$  parameterizations are shown in Fig. 10. Notations for evolution remain the same as in the previous pictures. This plot persuades that at high energies the hard pomeron effects cannot be neglected even for rather shallow column depths of matter. Pomeron effects, being raised in shadow factors into exponent, bring to tremendous changes as compared

with previous estimations. These coefficients are evidently the most sensitive observables in the  $HE$  neutrino astrophysics to the hypothetical hard pomeron enhancement of  $\nu N$  structure functions.

## Conclusions

In this paper we have studied different manifestations of hypothetical hard pomeron enhanced  $\nu N$  structure functions in the high-energy neutrino astrophysics. We have compared i) cross-sections  $\sigma_{\nu N}(E)$ , ii) rates of hadron-electromagnetic cascades, parametrized through differential and integral hadron moments,  $Z_h(E_h, \gamma)$ ,  $Y_h(E_h, \gamma)$ , and iii) shadow factors  $S(E_\nu, \tau)$ , calculated within hard pomeron enhanced  $DL+CTEQ5$  parameterization, with analogous values calculated within simple extrapolation of structure functions from high- $x$  perturbative  $QCD$  description to the low- $x$  region,  $Log + CTEQ5$ .

We found that these effects, if our assumption are justified, may change substantially our notion of high energy neutrino astrophysics. The most pronounced evidence for their presence has been found in the rapid decrease of shadow factors with energy. It may be seen even with column depths available at the Earth. We hope the validity of our suggestions will be checked by future giant neutrino telescopes.

## Acknowledgments

This research has been supported in part by the *INTAS* grant No: 99-1065.

## References

- [1] V. S. Berezinsky, S. V. Bulanov, V. A. Dogiel, V. L. Ginzburg and V. S. Ptuskin, *Astrophysics of Cosmic Rays* (North-Holland, Amsterdam, 1990).
- [2] KASCADE collaboration: H. O. Klages *et al.*, Nucl. Phys. (Proc. Suppl.) **52B**, 92 (1997).
- [3] T. Abu-Zayyad *et al.*, Proc. of 25th Int. Cosmic Ray Conf., Salt Lake City, Utah **3**, 264 (1999).

- [4] K. Greisen, *Phys. Rev. Lett.* **16**, 748 (1966).  
G. T. Zatsepin and V. A. Kuzmin, *Soviet Physics JETP Lett.* **3**, 78 (1966).
- [5] A. Z. Gazizov, in *Proc. of 8th Annual Seminar NPC'S'99*, edited by L. Babichev and V. Kuvshinov (Institute of Physics, Minsk, 2000), Vol. 8, p. 242.
- [6] D. J. Bird *et al.*, *Astrophys. Journ.* **424**, 491 (1994).
- [7] P. Sokolsky, in *Proc. of AIP Conference* (1998), p. 65.
- [8] O. Catalano *et al.*, in *Proc. of 19th Texas Symposium on Relativistic Astrophysics* (Paris, France, 1998).
- [9] The Pierre Auger Project Design Report, Fermilab (1995), see [www.auger.org](http://www.auger.org).
- [10] V. S. Berezhinsky, A. Z. Gazizov, G. T. Zatsepin and I. L. Rozental, *Sov. J. Nucl. Phys.* **43**, 637 (1986).
- [11] R. Gandhi, C. Quigg, M. H. Reno and I. Sarcevic, *Phys. Rev. D* **58**, 093009 (1998).
- [12] G. M. Frichter, D. W. McKay and J. P. Ralston, *Phys. Rev. Lett.* **74**, 1508 (1995).
- [13] J. Kwiecinski, A. D. Martin and A. M. Stasto, *Acta Phys. Polon.* **B31**, 904 (2000).
- [14] A. Z. Gazizov and S. I. Yanush, in *Proc. of 9th Annual Seminar NPC'S'2000*, edited by L. Babichev and V. Kuvshinov (Institute of Physics, Minsk, 2000), Vol. 9, p. 313.
- [15] A. Z. Gazizov and S. I. Yanush, *Phys. Rev. D* (2002), (in press); astro-ph/0105368.
- [16] H1: C. Adloff *et al.*, *Nucl. Phys.* **B497**, 3 (1997).  
H1: C. Adloff *et al.*, *Eur. Phys. J.* **C21**, 33 (2001).  
ZEUS: J. Breitweg *et al.*, *Phys. Lett.* **407B**, 432 (1997).

- [17] A. Donnachie and P. V. Landshoff, Phys. Lett. **437B**, 408 (1998).  
A. Donnachie and P. V. Landshoff, Phys. Lett. **B**, (in press); hep-ph/0105088.  
A. Donnachie and P. V. Landshoff, hep-ph/0111427.
- [18] E. A. Kuraev, L. N. Lipatov and V. S. Fadin, Sov. Phys. JETP **45**, 199 (1977).  
Y. Y. Balitzkij and L. N. Lipatov, Sov. J. Nucl. Phys. **28**, 822 (1978).
- [19] CTEQ collaboration: H. L. La *et al.*, hep-ph/9903282; see also <http://www.phys.psu.edu/~cteq/>.
- [20] V. S. Berezinsky and A. Z. Gazizov, Sov. J. Nucl. Phys. **29**, 1589 (1979).
- [21] V. S. Berezinsky and A. Z. Gazizov, in *Proc. of 1979 DUMAND Summer Workshop at Khabarovsk and Lake Baikal* (Hawaii, Honolulu, 1980), p. 202.
- [22] A. Z. Gazizov and S. I. Yanush, in *Proc. of 10th Annual Seminar NPC'S'2000*, edited by L. Babichev and V. Kuvshinov (Institute of Physics, Minsk, 2001), Vol. 10, p. 334.
- [23] A. Nicolaidis and A. Taramopoulos, Phys. Lett. **B386**, 211 (1996).
- [24] V. A. Naumov and L. Perrone, Astropart. Phys. **10**, 239 (1999).